Three-Mirror Off-Axis Anastigmats for CMB Surveys

Mike Lampton
UCBerkeley Space Sciences Lab
mlampton@SSL.berkeley.edu
www.MikeLampton.com
www.StellarSoftware.com

October 29, 2016

1 Introduction

Three-mirror-anastigmat telescopes have enough design parameters (spacings, curvatures, and conic constants) to simultaneously zero or minimize all the principal optical aberrations For an overview of TMAs, see P.N.Robb, Appl. Optics v17 #7 2677 1978. The two alternative designs of the TMA are the four on-axis layouts pioneered by Dietrich Korsch, and the off-axis designs developed by Lacy Cook (L.G. Cook, Proc SPIE v.183 1979).

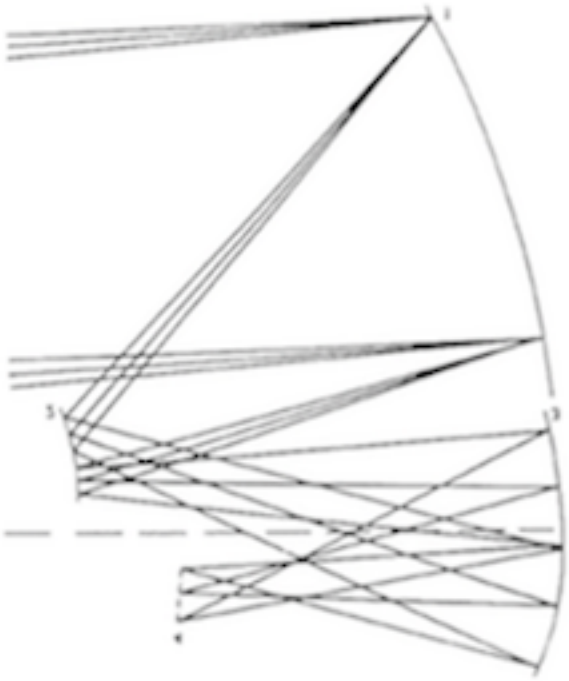

Figure 1: An f/2.5 TMA, from Cook 1979 figure 1.

Here I present two instantiations of the Cook-type three mirror anastigmat telescope that are potentially suited for CMB survey work. These are fully off-axis so that the diffraction effects of a central pupil obscuration do not occur. They each also have, in common with the Cook concept, an exit pupil that is exterior to the converging light within the telescope, so that a cold stop can be located at the exit pupil to block heat from the edges of the primary mirror. (You will recall that the exit pupil is an image of the entrance pupil, and is commonly used to limit the working size of the effective primary mirror, thereby limiting its diffraction edge effects and stray heat.)

These two examples have not been optimized in the sense of supplying detailed polynomial coefficients and toric properties of the three mirrors. Instead these use only the properties of conic sections of revolution, that help provide a starting point for detailed future optimization. However the performance is already attractive and should be considered within the trade space of future CMB imagers.

2 First Example: Cook13

```
  4 surfaces    Cook13.OPT   pupil centered   FL=15m, f/2.5, D=6m.     422umRMS
    X,m       Z,m    pitch,deg    Type?     Curvature    Aspher    OffOx    Form
----------:---------:---.------:---------:---.--------:----------:--------:------:---
  -6.33505?   0     : -4.5     : Mir,pri : -0.05504251? -0.751030?  6.3   :      :
  -5.55916? -8.5    : -1       : Mir,sec : -0.17360534? -9.262363?  1.1   :      :
  -5.59268? -0.5    :  0.815060: Mir,ter : -0.12839545? -0.106060? -0.9   :Square:
  -6.8    : -8.82500? -0.250758: Focus   :            :          :        :Square:
          :         :          :         :            :          :        :      :
```

Design parameters held fixed were these:

- pupil: 6m diameter filled circle
- focal length: 15 m, hence f/2.5
- optimized working field: 3x3 degrees = 780mm square

This first example, identified here by its filename Cook13, was arrived at by starting with a fully coaxial but off-axis-illuminated TMA, and allowing the curvatures and asphericities to float under the BEAM FOUR autoadustment nonlinear minimum least squares (Levenberg-Marquardt) algorithm. The final plate scale was kept fixed, and the locations of the mirror vertices were initially also fixed. A sequence of increasing number of autoadjustments was employed, with eventual freedom for the surface displacements (X in the table) and pitch angles (Pitch in the table). Enforcement of the exposure of the exit pupil had to be managed manually by restricting the primary mirror pitch angle.

The coordinate system used here is Cartesian, with optical surface vertex locations in meters shown in the table BEAM FOUR optics definition file shown above. Items with question mark tags are selected for autoadjustment, while the other parameters are held fixed. Asphericities are zero for spheres, or $-1 < A < 0$ for ellipsoids, $A = -1$ for paraboloids, and $A < -1$ for hyperboloids. As usual for TMAs, the primary and tertiary mirrors must be ellipsoids, while the secondary must be a strong hyperboloid. These work off axis by the distances shown in their "OffOx" column.

What is specific to Cook13 is the choice of optimization field. Here, I have assumed that the best image quality ought to be obtained over the central 3x3 degree field, with the image quality unconstrained outside this field. Within this field, optimization of the marked parameters gives a net RMS blur (1D, circular) of 422microns. We can expect the edges of the 3x6 degree field to be much poorer since they had no vote in managing the optical surfaces.

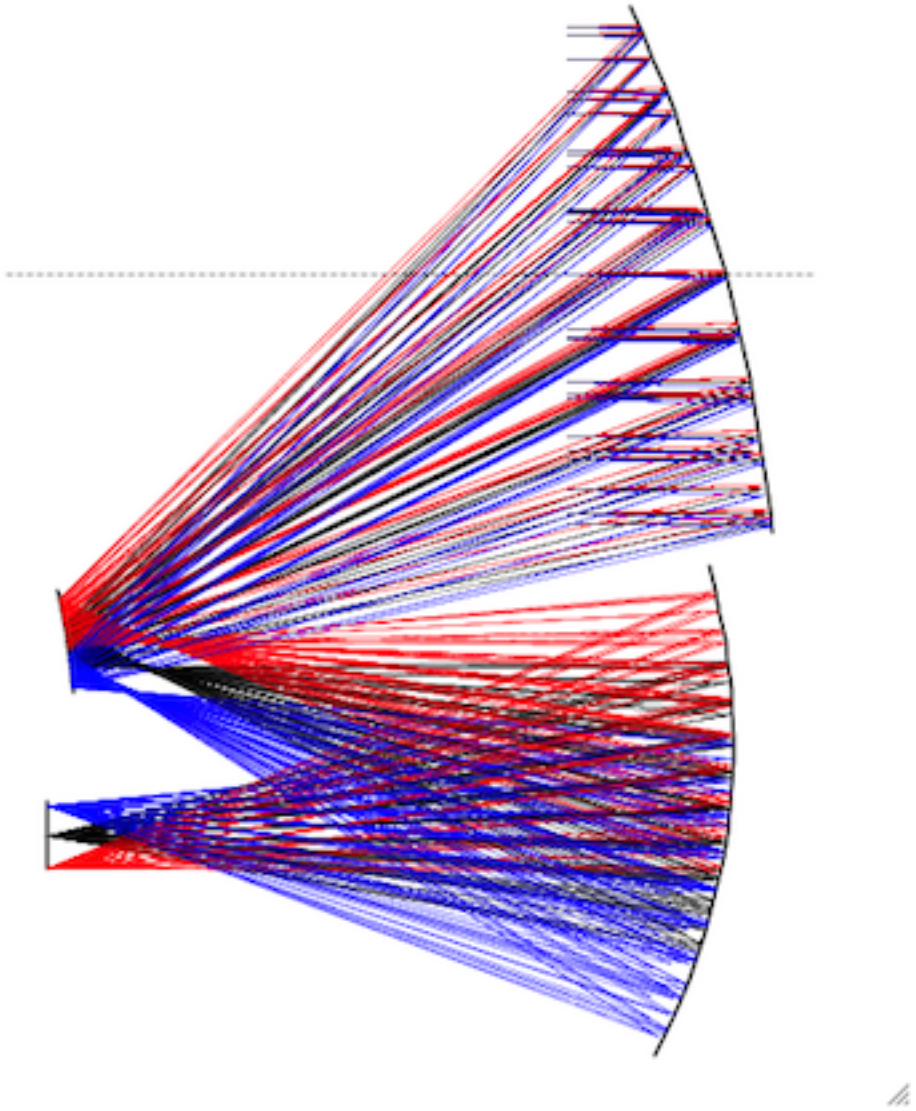

Figure 2: Cook13 side view.

In Figure 3, I show the spot diagram of Cook13, on a 1 degree grid, 6 degrees wide and 3 deg tall. The optical axis lies just above the top center of the diagram. The field edges are obviously much more poorly focussed; they were not part of the optimization. However the

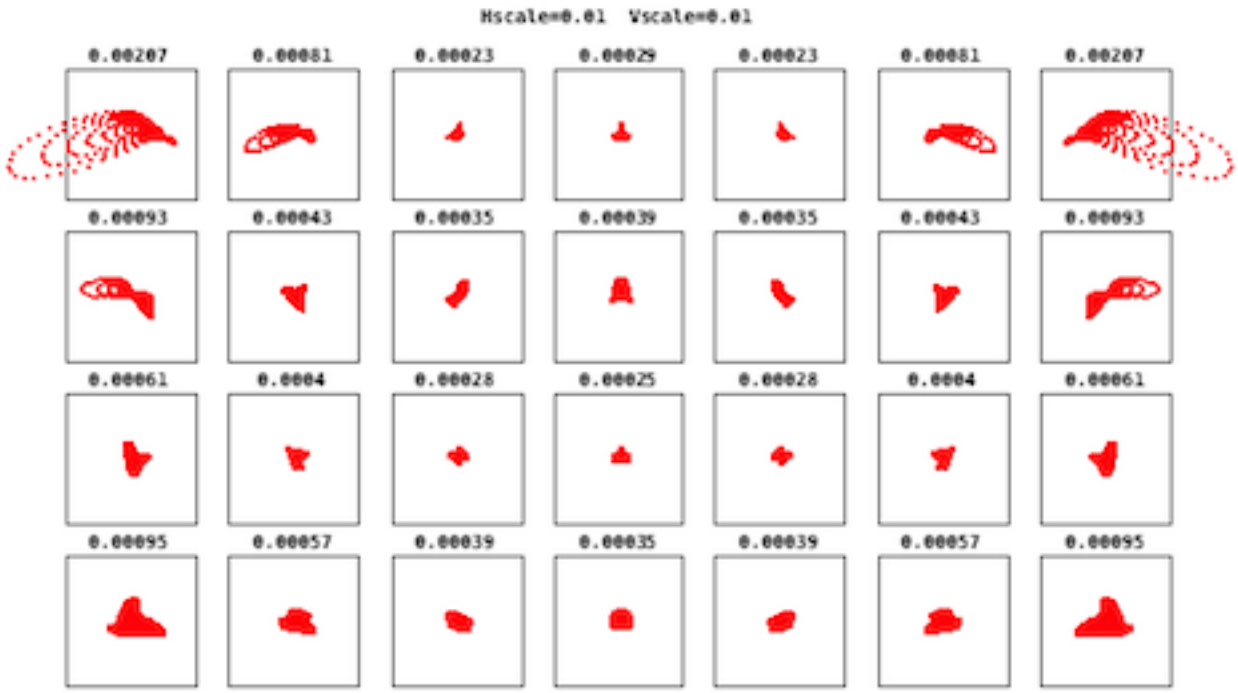

Figure 3: Cook13 spot diagram, 1 degree grid, 3x6 degree field, 10mm box size with rms spot sizes in meters.

central part of the field is very good: typical blur is of the order of 300 microns RMS, and the 3x3 field average is 422 microns RMS.

3 Second Example: Cook14

This example is just like the previous "Cook13" case, same 6 meter diameter pupil, same f/2.5 focal ratio and same 15 meter focal length. However here I included all the field points in the 3x6 degree field as contributors to the optimization. Enlarging this optimization region makes the 3x6 degree field more homogeneous.

```
  4 surfaces    Cook14.OPT   pupil centered   FL=15m, f/2.5, D=6m.     835umRMS
    X,m     Z,m      pitch,deg   Type?     Curvature     Asph     Dx   OffOx    Form
----------:---------:---.-----:---------:---.--------:---.------:---:--------:------:---
  -6.35536?   0     : -4.5    : Mir,pri : -0.05488895? -0.743853?   :  6.3   :      :
  -5.59642? -8.5    : -1      : Mir,sec : -0.16404557? -8.293249?   :  1.1   :      :
  -5.57979? -0.5    :  1      : Mir,ter : -0.12929658? -0.105919? 6 : -0.9   :Square:
  -6.8    : -8.73521?  0      : Focus   :             :           :   :        :Square:
          :         :         :         :             :           :   :        :      :
```

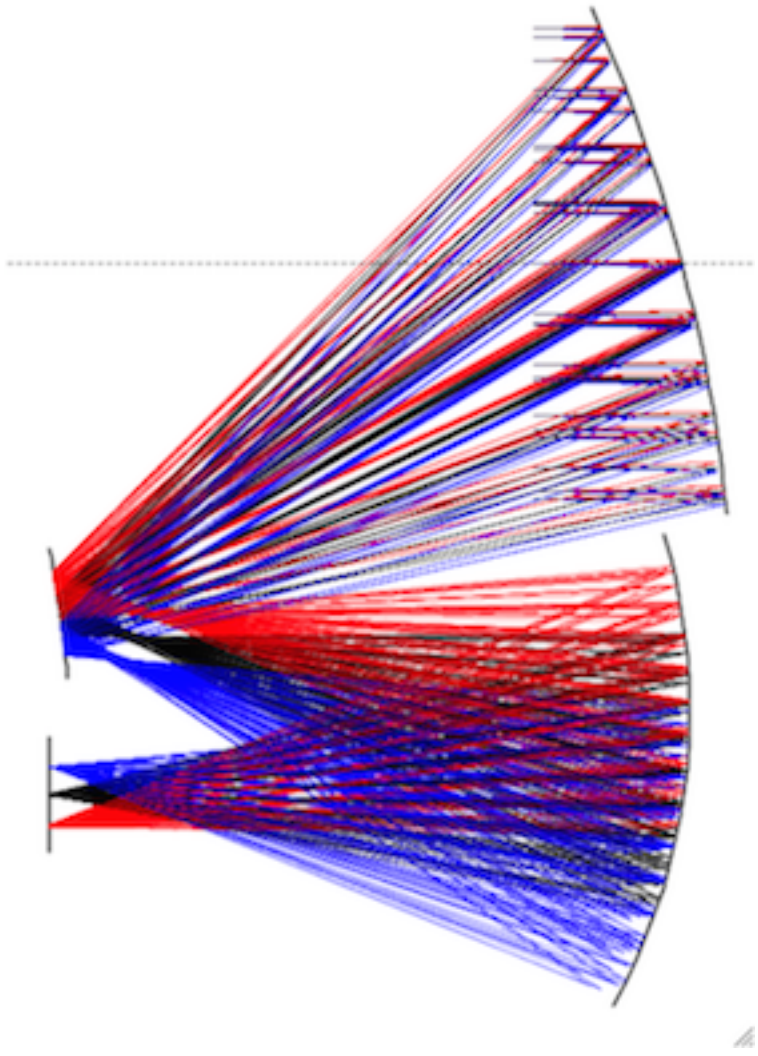

Figure 4: Cook14 side view.

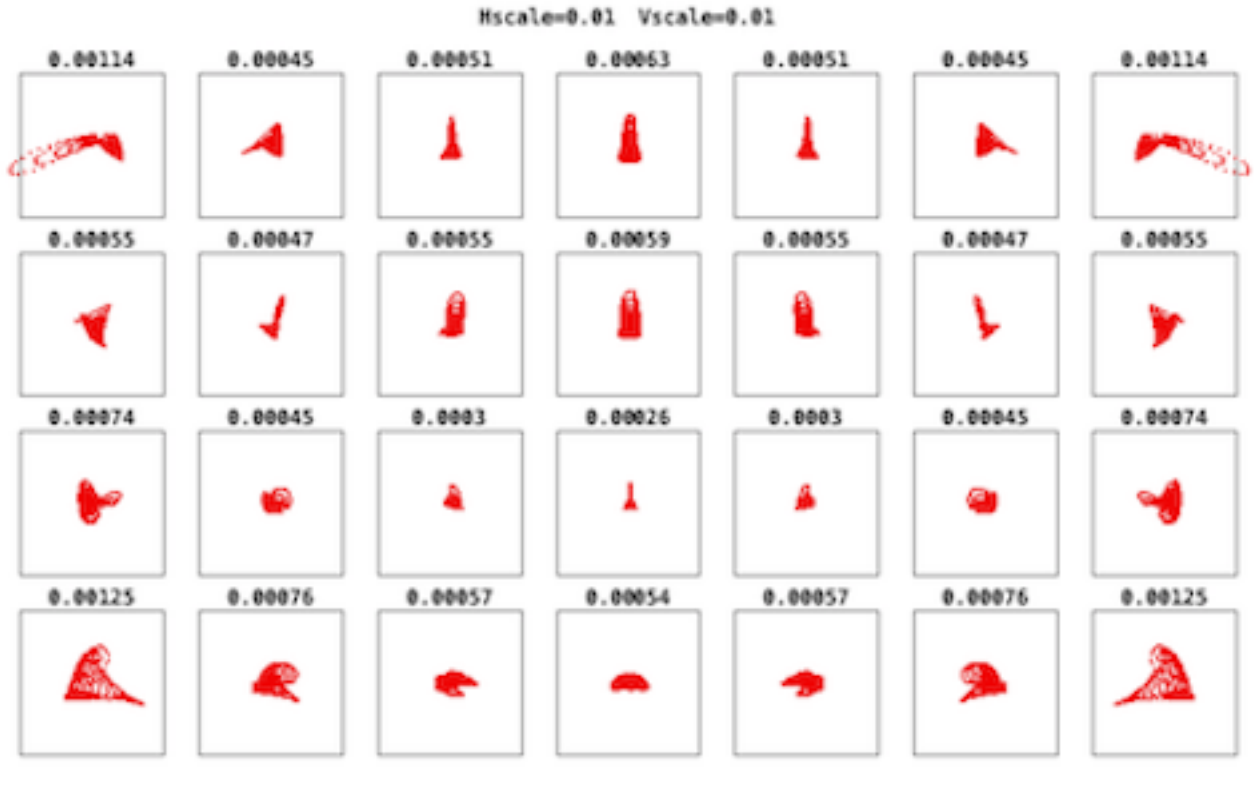

Figure 5: Cook14 spot diagram. 10mm boxes spanning 3x6 degree field.

4 PSF Sizes and Strehl Ratios

The Strehl ratio is defined as the ratio of the aberrated peak point spread function (PSF) to the unaberrated peak point spread function. In Fourier space, the the modulation transfer function (MTF) conveys the same information: its integral over all spatial frequencies controls the peak intensity. The Strehl ratio for an aberrated MTF is the ratio of its frequency-weighted MTF integral to the unaberrated integral.

In three-mirror anastigmats, all the primary aberrations (coma, spherical, curvature of the field) have been zeroed, or more precisely reduced to minimize the size of the PSF over a given field. For this reason, TMA aberrations are always bizarre looking: we cannot visually identify any familiar aberrations but see only an ungainly mess of higher aberrations mixed together.

Instead of Bessel transforming these individual bizarre shapes, I have chosen a quick approximate way to estimate the Strehl ratio variation over the TMA fields. The spot diagrams give the second moments of the spots. Here, I calculate the (easy) integral of aberrated MTF for a general circular Gaussian blur, and choose that Gaussian that has the same second moment as the ugly TMA aberration combination seen at each field point. Having mapped the rms blurs over the field, I use the appropriately sized Gaussian Strehl

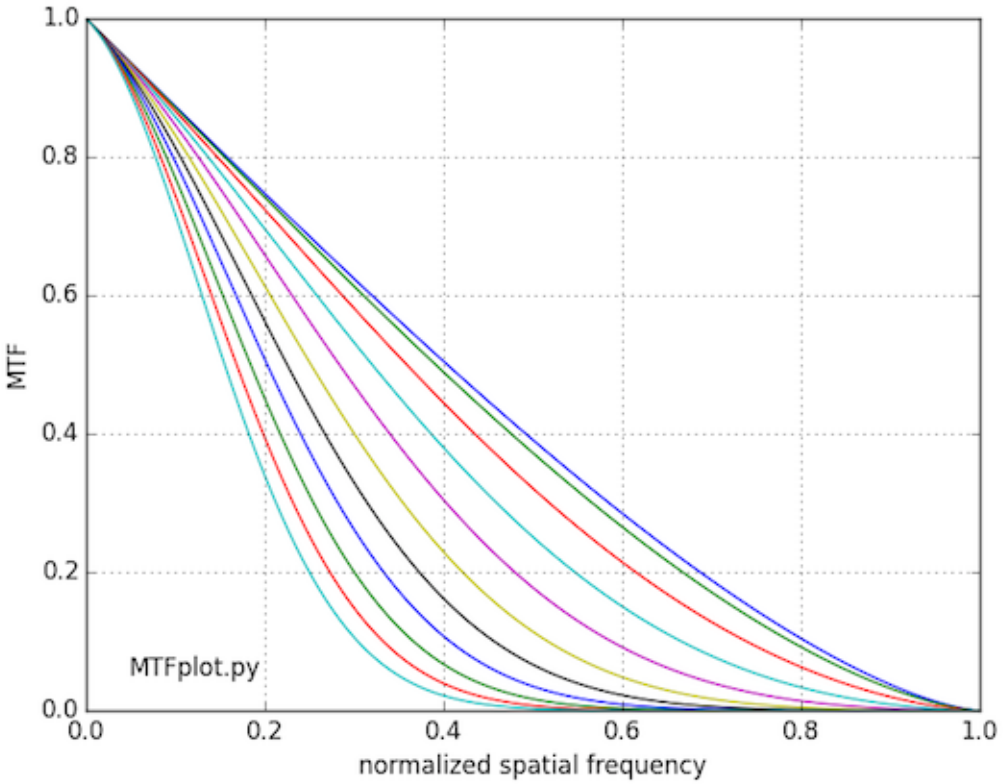

Figure 6: MTF for circular pupil with Gaussian aberration with $\sigma = 0., 0.1, ...1.0$ where σ is the angular rms radius of the Gaussian, normalized to the cutoff angle λ/D. The Strehl ratio is the area under each curve compared to the unaberrated curve area. As the blur rises, the Strehl ratio falls monotonically.

as an estimate of the TMA Strehl map.

Briefly, the unaberrated and aberrated MTFs and Strehl ratio are given by the expressions

$$MTF(f,0) = \frac{2}{\pi}\left(arccos(f) - f\sqrt{1-f^2}\right) \tag{1}$$

$$MTF(f,\sigma) = MTF(f,0) \cdot exp(-2\pi^2\sigma^2 f^2) \tag{2}$$

$$Strehl(\sigma) = \frac{\int_0^1 MTF(f,\sigma) f df}{\int_0^1 MTF(f,0) f df} \tag{3}$$

where the first expression can be found in Schroeder D.J., "Astronomical Optics',' 2nd edition p.283, and the second expression is from Schroeder p. 288 or Mahajan V.N., "Aberration Theory," SPIE Press 2011. Here, f is the spatial angular frequency normalized to the diffraction cutoff frequency D/λ and the Gaussian rms blur angle σ is similarly normalized to λ/D. The spatial frequency f appears within the Strehl integral as part of the Bessel transform from the one dimensional MTF representation to the two-dimensional PSF representation.

For spreadsheet work, a simplified approximation to this Strehl function will be useful.

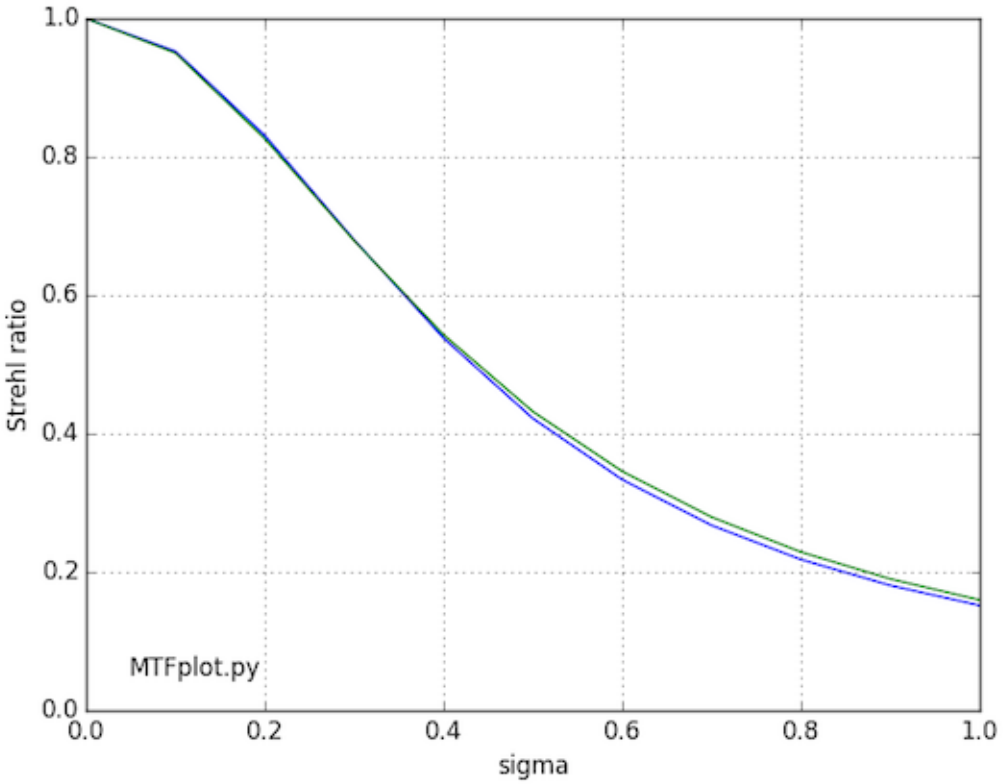

Figure 7: Blue curve: Strehl ratio for Gaussian blurs. Green curve: $1/(1 + 5.26\sigma^2)$ approximation.

In the work below I have integrated this family of MTF curves and plotted the Strehl ratios that each represents. I adopted the approximation shown in Figure 7, and applied this to the blur maps obtained from the spot diagrams to show the variation over a 3x6 degree field of view. Figure 8 below shows the Strehl maps at 300, 200, and 100GHz for Cook13. Figure 9 below shows the Strehl maps at 300, 200, and 100GHz for Cook14.

	Sigma, in millimeters						
degrees	-3	-2	-1	0	1	2	3
1.5	2.07	0.81	0.23	0.29	0.23	0.81	2.07
0.5	0.93	0.43	0.35	0.39	0.35	0.43	0.93
-0.5	0.61	0.41	0.28	0.25	0.28	0.41	0.61
-1.5	0.95	0.57	0.39	0.35	0.39	0.57	0.95
300	GHz, λ=	1.00	mm				
	Approximate Strehl at this wavelength						
	0.22	0.64	0.96	0.93	0.96	0.64	0.22
	0.56	0.73	0.77	0.75	0.77	0.73	0.56
	0.66	0.74	0.81	0.83	0.81	0.74	0.66
	0.56	0.68	0.75	0.77	0.75	0.68	0.56
200	GHz, λ=	1.500	mm				
	Approximate Strehl at this wavelength						
	0.38	0.80	0.98	0.97	0.98	0.80	0.38
	0.76	0.94	0.96	0.95	0.96	0.94	0.76
	0.88	0.94	0.97	0.98	0.97	0.94	0.88
	0.75	0.89	0.95	0.96	0.95	0.89	0.75
100	GHz, λ=	3.00	mm				
	Approximate Strehl at this wavelength						
	0.71	0.94	1.00	0.99	1.00	0.94	0.71
	0.93	0.98	0.99	0.99	0.99	0.98	0.93
	0.97	0.98	0.99	0.99	0.99	0.98	0.97
	0.92	0.97	0.99	0.99	0.99	0.97	0.92

Figure 8: Strehl maps for Cook13

	Sigma, in millimeters						
degrees	-3	-2	-1	0	1	2	3
1.5	1.14	0.45	0.51	0.63	0.51	0.45	1.14
0.5	0.55	0.47	0.55	0.59	0.55	0.47	0.55
-0.5	0.74	0.45	0.23	0.26	0.23	0.45	0.74
-1.5	1.25	0.76	0.57	0.54	0.57	0.76	1.25
300	GHz, λ=	1.00	mm				
	Approximate Strehl at this wavelength						
	0.48	0.85	0.82	0.75	0.82	0.85	0.48
	0.80	0.84	0.80	0.77	0.80	0.84	0.80
	0.68	0.85	0.96	0.95	0.96	0.85	0.68
	0.43	0.67	0.79	0.80	0.79	0.67	0.43
200	GHz, λ=	1.500	mm				
	Approximate Strehl at this wavelength						
	0.67	0.93	0.91	0.87	0.91	0.93	0.67
	0.90	0.92	0.90	0.88	0.90	0.92	0.90
	0.83	0.93	0.98	0.98	0.98	0.93	0.83
	0.63	0.82	0.89	0.90	0.89	0.82	0.63
100	GHz, λ=	3.00	mm				
	Approximate Strehl at this wavelength						
	0.89	0.98	0.98	0.96	0.98	0.98	0.89
	0.97	0.98	0.97	0.97	0.97	0.98	0.97
	0.95	0.98	1.00	0.99	1.00	0.98	0.95
	0.87	0.95	0.97	0.97	0.97	0.95	0.87

Figure 9: Strehl maps for Cook14.

4.1 Concluding Remark

Seems to me that additional work could usefully be done to reduce the most annoying feature of these example TMAs: the tertiary mirrors are huge! As big as the primary mirror, and wider, for the unvignetted 3x6 field case. If the tertiary could be brought closer to the secondary, its working size would be somewhat reduced. But my efforts so far cause considerably larger blur. Plenty more work to be done!